Parametric Study of the Flow Characteristics and Heat Transfer from Intermittent Circular Jet Impinging on a Concave Surface

Saeed Rakhsha, Mehran Rajabi Zargarabadi*, Seyfollah Saedodin

Faculty of Mechanical Engineering, Semnan University, P.O.B. 35131-191, Semnan, Iran.

PAPER INFO	ABSTRACT
	The main purpose of the current work is the analysis of the pulsating effect on the flow and heat transfer from impinging jet on a concave surface. In this way, the heat flux of 2300 W/m² has been applied constantly on the surface with a radius of 120mm. The intermittent jet has been created for the frequency range of 1-100Hz by the pulsed-jet generator. Nusselt number distribution and flow field have been investigated for a dimensionless distance of the nozzle to surface (H/d) 2 to 5 and Reynolds number from 7000 to13000. The comparison of the experimental data with Numerical simulation shows that the k-ε RNG turbulence model is appropriately capable of predicting the Nusselt number on the concave surface under the pulsed jet impinging. Results of the present research indicate that pulsating the jet is more effective on the concave surface than the flat surface. Also, as compared to steady jet, when pulsating applies to the inlet jet with low frequency, reduction in Nusselt number is acquired. Furthermore, at each Re number and H/d, a threshold Strouhal number is found above which the Nusselt number of the pulsed jet is greater than that of the steady jet. Moreover, for the low nozzle to surface distance, Nu of stagnation point at low and high frequency varies with $Sr^{0.05}$ and $Sr^{0.15}$, respectively. At Re=10000, pulsating the impinging jet with f =100Hz causes an increase in the time and area-averaged of Nusselt number by 22% and 20% in comparison to steady jet at H/d=5 and 2, respectively.

1. Introduction

Jet impinging has been offered as a powerful technique for the high heat transfer rate. It has a variety of applications, including heating, cooling, and drying of electronic devices, turbomachinery, and other industries. Many studies have been carried out to investigate the flow structure and heat transfer of the impinging jet [1-5]. Pulsating the impinging jet is a popular way to increase the efficiency of heat transfer through changing the flow structure. Numerous research works have been applied on the flow characteristic and heat transfer of pulsed jet impinging [6-9]. Sailor et al. [10] used 0.009<Sr<0.042 to perform the experiment. They showed that a significant enhancement in heat transfer rate from the impinging surface is there. Kumar et al. [11] simulated the heat and flow field of pulsed laminar flow using a numerical method. The following parameters were considered:

Reynolds number (100<Re<1000), frequency of oscillating (1<f<20), and distance between the nozzle and impinging surface. Xu et al. [12] modeled the oscillated turbulent flow using the numerical method. They concluded that fluctuating flow has little impact on heat transfer. Bejera et al. [13] found that the sinusoidal pulsating caused the increase in heat transfer of impinging jet. Zhou et al. [14] studied the heat transfer of sinusoidal and step functions impinging jet by experimental investigation. According to their result, at the smooth surface, the sinusoidal jet increases the heat transfer by 10% while the step jet increases it by 40%. Kurnia et al. [15] evaluate the efficiency of a dryer using intermittent jet impinging. They concluded that the intermittent jet reduces the dryer rate in comparison to the steady jet. Poh et al. [16] attempted the heat transfer of the step pulsed jet using a numerical approach. Impact of Reynolds number,

**Corresponding Author: Mehran Rajabi Zargarabadi, Faculty of Mechanical Engineering, Semnan University, P.O.B. 35131-191, Semnan, Iran.*
Email: rajabi@semnan.ac.ir

the temperature difference among impinging surface and inlet jet, the distance between surface, and nozzle and frequency of swinging jet have been investigated. Middelberg and Herwig [17] investigated the heat transfer of the pulsed impinging jet for the different pulsed functions through the experiments. They concluded that low-frequency pulsed jet reduces the heat transfer for all of the functions in the stagnation region. Zulkifli and Sopian [18], by experimental investigation, showed that the local Nusselt number of the pulsed jet is greater than the steady jet in the wall jet area. Mohammad pour et al. [19] attempted to find the optimized arrangement of the steady and pulsed jets on a flat surface through numerical simulation. Hosseinalipour et al. [20] found that pulsating the jet with low frequency can't lead to an improvement in the heat transfer rate from the plate.

According to the literature, it can be said that the presence of a secondary flow on the concave surface leads to an improvement in the heat transfer rate of the impinging jet [21-23]. Hashiehbaf et al. [24] investigated the turbulent jet impingement on the concave surface by performing the experiments. They showed that a strong lateral movement has been created by the concave surface. They also indicated that the flow has strength turbulence intensity near the concave surface compared to the flat one. Mohammad pour et al. [25] conducted the two-dimensional simulation of the flow characteristic and heat transfer of the pulsed impinging jet on the concave surface. Rajabi et al. [26] attempted to simulate heat transfer and turbulent flow of pulsed jet impinging on the asymmetric concave surface. The effect of the array arrangement of multi-jet impinging on the concave surface has been studied by Dandan et al. [27]. They found that both inline and staggered arrangements improve the heat transfer in comparison to the array jet.

Regarding the literature, No experimental study is available for pulsed-jet impinging on heated concave surfaces. In this paper, it has been focused on the respective experimental investigation on the concave surface. Accordingly, the effect of pulse frequency, nozzle to surface distance, and Reynolds number on the Nusselt distribution have been experimentally investigated. A three-dimensional simulation has been implemented to understand the effect of pulsating jet and the concave surface on the flow characteristic of the impinging jet. It should be noted that previous numerical investigations have been carried out two-dimensionally.

2. Experiments

As Fig. 1 shows, the setup contains an air compressor, temperature sensors, pressure gauge, ball valve, pulsed-jet generator, reservoir, and a concave surface with constant heat flux. The inlet flow rate is controlled by a ball valve to adjust the specific velocity and Reynolds number. The pulsed jet generator has been manufactured using a rotating disc that has been cut off as two arcs of 90 degrees symmetrically (see Fig .2). When An AC motor drives the disc with a specific frequency from 1-200 Hz, the

frequency of the pulsed- jet is two times to velocity of the disc. An electronic motor controller is there to regulate the speed or frequency of the disc. When the disc rotates airflow path is blocked and connected. Thus step velocity profile has been generated. The velocity profiles have been measured by a pitote tube which was calibrated with a micro-manometer which is equipped with an A/D card and time response of millisecond. Regarding the time response of the pitote tube, the oscillation of velocity cannot be detected at high frequency. Therefore, the pulse generator was examined at a low frequency of the pulsed jet and data was recorded on the storage card. By plotting the recording data, the pulsed velocity profile was obtained as Fig.3. The components of the concave surface are shown in Fig 4. The concave surface has been painted with black spray paint. The spray paint is stored in a pressure vessel and is spread using a valve to release a mixture of compressed air and paint. The result is a fine layer (0.01-0.03 mm thickness) used for various types of surfaces. As shown in Fig.4, a silicon rubber heater has been applied on the bottom of the concave surface to implement the constant heat flux of 2300 W/m². The heater module is insulated with two layers of glass wool and rock wool to minimize the heat loss from the convex surface.

The temperature distribution along the concave surface has been measured by an IR camera. The test surface is covered with high emissivity black paint to permit temperature measurement by a thermal infrared camera. Before measuring surface temperature, the IR camera should be calibrated. A K-type thermocouple was used to ensure the calibration of the IR camera. The concave surface was heated with a silicon heater continuously until the steady-state was established. When the temperature of the target surface drops gradually, the temperature of the concave surface is recorded by both the IR camera and the thermocouple. Given the surface temperature, the Nusselt number can be calculated as follows:

$$Nu = \frac{q''}{T_s - T_{jet}} \left(\frac{d}{K}\right) \qquad (1)$$

The experiments were performed for four jet-to-surface distances of (2.0, 3.0, 4.0, and 5.0) and five Reynolds numbers (7000, 8000, 10000, 11500 and 13000). The uncertainty of experiments can be calculated by recognizing the significant sources of the errors. The uncertainty of each variable included systematic and random uncertainty. Therefore the overall uncertainty can be computed from the below equation:

$$\varepsilon_t = \pm\sqrt{\varepsilon_r{}^2 + \varepsilon_s{}^2} \qquad (2)$$

Which ε_s and ε_r are systematic and random errors. To achieve the repeatability of experimental data, the experiments were performed three times. The random error of the Nusselt number has been obtained from the least mean square by ±7.4%. The systematic errors of the measuring parameters have been presented in Table 1. The accuracy for temperature measurement is about 0.5 ⁰C.

(1) Air Compressor
(2) Reservior
(3) Control Box
(4) Ball Valve
(5) Pressure Gauge
(6) Pulsed Generator
(7) Frequency Controller
(8) DC Electerical Motor
(9) Pitot Tube
(10) Thermal Camera
(11) A/D Card
(12) PC
(13) Concave Surface
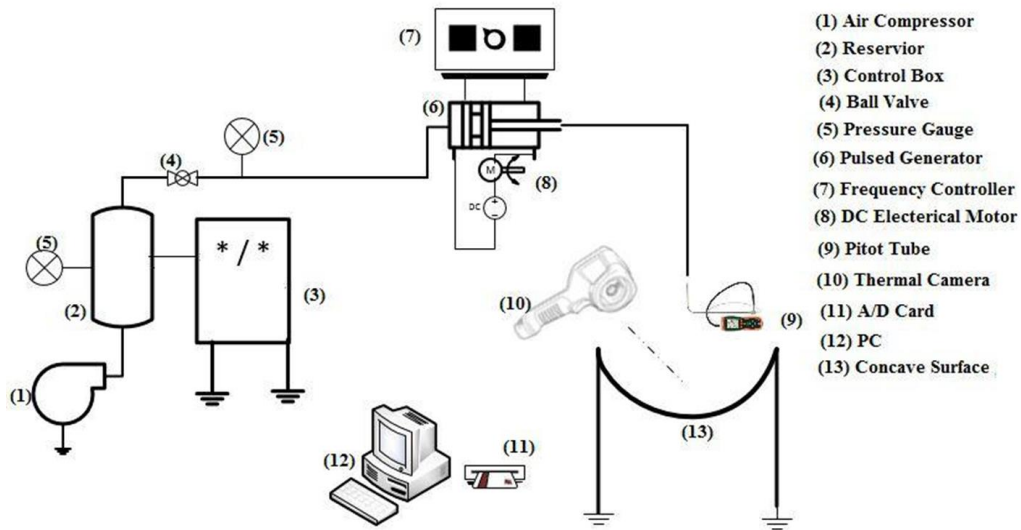
Figure 1. A schematic view of the experimental setup

(1) Inlet Connection
(2) Rotating Disc
(3) Outlet Connection
(4) AC Motor
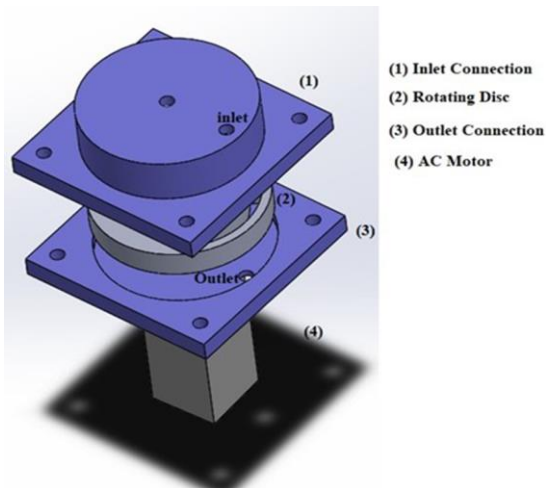
Figure 2. 3D model with a part list of the setup of pulsed-jet generator

(1) Concave Surface
(2) Silicon heater
(3) Rock-wool
(4) Glass wool
(5) Convex Surface
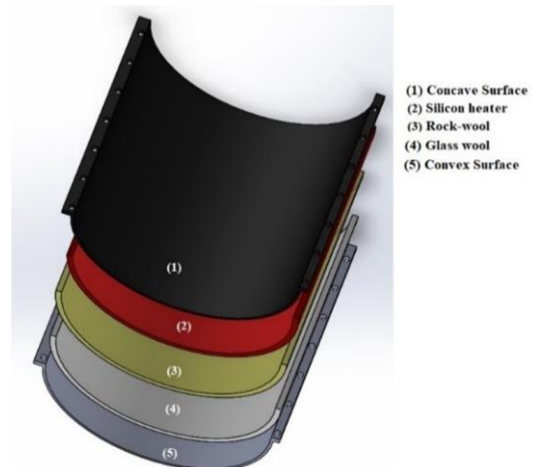
Figure 4. Schematic view of the concave surface and Components

According to the experimental result, the heat loss due to natural convection is approximately smaller than 1% of the implemented heat flux. The heat losses because of radiation would be calculated as less than 1%. The systematic error of the Nusselt number can be obtained by the root-sum-square combination of components. The systematic error has been computed by ±9% for the Nusselt number. The overall uncertainties for the Nusselt number is about ±11.7% using the eq. 2.

Figure 3. The velocity distribution of pulsed jet Re=14000

Table 1. The error of measuring instrument.

Instruments	Range of errors
Power supply	±1.5% F.S
Pitot tube	±0.3% F.S
IR camera	±(2.3+2.5% rdg)
K-type thermocouple	±0.5 ^{0}C

3.   Numerical method

The study of flow characteristics of the pulsed impinging jet can help understand the effect of pulsating on the heat transfer rate from the concave surface; hence the numerical solution is used to explain the experimental observation. The numerical method has been performed for the various range of pulsed jet frequency (1 Hz to 100 Hz), Nozzle to surface distance (H/d=2 to H/d=5), and Re=7000 to 13000.

3.1. Governing Equation

The governing equations of the present problem are the transient form of continuity, momentum, and energy equation. Relations 3 to 5 define the corresponding equations.

$$\frac{\partial \rho}{\partial t} + \frac{\partial (\bar{u}_i)}{\partial x_i} = 0 \tag{3}$$

$$\frac{\partial (\rho \bar{u}_i)}{\partial t} + \frac{\partial (\rho \bar{u}_i \bar{u}_j)}{\partial x_j} =$$
$$-\frac{\partial \bar{P}}{\partial x_i} + \frac{\partial}{\partial x_j}\left[\mu\left(\frac{\partial \bar{u}_i}{\partial x_j} + \frac{\partial \bar{u}_j}{\partial x_i}\right) - \rho\overline{u_i'u_j'}\right] \tag{4}$$

$$\frac{\partial (\rho C_p \bar{T})}{\partial t} + \frac{\partial (\rho C_p \bar{u}_i \bar{T})}{\partial x_i} =$$
$$\frac{\partial}{\partial x_i}\left(k \frac{\partial \bar{T}}{\partial x_i} - \rho C_p \overline{u_i'T'}\right) \tag{5}$$

The terms $\rho \bar{u}_i \bar{u}_j$ and $\rho C_p \overline{u_i'T'}$ can be modeled by the turbulence models. The prediction capability of the turbulence models has been studied, such as LES [29] and RANS [30] for impingement heat transfer. Previous researchers [30-32] have declared that the RNG k-ε is a suitable model to predict the flow and thermal characteristics of impinging jets. Therefore the RNG k-ε model is applied for modeling the turbulence in both steady and pulsed jets. As regards impinging flows, as the jet hits to the surface, the stagnation region has been produced, that the Reynolds number is reduced drastically. Although the k– ε model is qualified for high Reynolds flow, for the RNG model, the differential expression has been derived to predict the low Reynolds flows. However, the efficiency of this model depends on the near-wall function and mesh refinement on the boundary wall. It should be mentioned that the RNG k– ε cannot model the laminar to turbulent transition. In the present work, due to the high entrainment rate of the pulsed jet, the transition occurs before the impinging to the surface and doesn't happen on the wall jet region.

3.2. Geometry and Boundary Conditions

Geometry and computational domain have been shown in Fig.5a. The Geometry includes a concave surface and a single circular jet placed at a constant distance to the impinging surface. The concave surface was in a semi-cylindrical shape with a 240mm diameter and 320mm length. The nozzle diameter of the circular jet was 12mm.

As presented in the table.2, Velocity inlet was implemented for boundary inlet. The magnitude of inlet velocity was dependent on the Reynolds range of this study. The boundary conditions of the concave surface are no-slip for velocity and constant heat flux of 2300 W/m² for heat transfer. The fluid in this study is air as a Newtonian fluid. For calculating the Nu number, thermophysical properties have been extracted at the temperature of 330 K, which is the bulk temperature of airflow. Regarding the transient problem of the pulsating jet, the initial condition for governing equation has been considered as follows:

$u=v=w=0, \ \ P=P\infty, \ T=T\infty, \ \ k=\varepsilon=0$

Table 2. The Boundary condition for the numerical solution

Inlet	Velocity inlet: 8-24 m/s
	Inlet temperature: 300K
	Turbulence intensity: 3-10%
	Turbulence kinetic energy :0.24 m²/s²
Outlet	Pressure Outlet: Atmosphere-0 bar G
Concave surface	Constant heat flux-2300 W/m² No-slip condition

The velocity profile of intermittent jet is described as:

$$\frac{u_{jet}}{u_{ave}} = 2.0 \rightarrow n \ll \frac{t}{T} < \frac{(2n+1)}{2}$$

$$(n=0, 1, 2, 3,...) \tag{6}$$

$$\frac{u_{jet}}{u_{ave}} = 0.0 \rightarrow \frac{(2n+1)}{2} \ll \frac{t}{T} < n$$

3.3. Numerical Procedure

Figure 5. b illustrates the structured and non-uniformed grid of the simulation domain. For the investigation of the mesh independence, four different grid sizes have been performed. Four grids have been generated by 956882, 1149355, 1511928, and 1773629 cells. By a comparison of the result of the complete simulation for four grids, the mesh with 1511925 cell numbers was selected to continue the research. As it is magnified in the figure, to improve the efficiency of the turbulence model, more grid are produced close to the wall to ensure Y⁺<1. According to the figure, in the area of impinging of the circular jet with the concave surface, a structured grid has been created so that the quality of the mesh in this area is of good quality.

The governing equations are discretized using the control volume approach [33]. For discretization of the advection term, the second-order upwind is applied. The solution algorithm for the coupling of pressure-velocity is SIMPLE-C. The time-dependent terms are discretized with the second-order implicit scheme. To ensure to detect the jet velocity fluctuation, the time-step is chosen τ/40 =1/40f. The convergence criterion is 10^{-6} for energy equations and 10^{-4} for continuity and momentum.

4. Result and Discussion

The time-averaged of local Nusselt number for a period of the pulsation is presented as follows:

$$Nu(x.s) = \frac{1}{T}\int_{t=0}^{t=T} Nu(x.s.t)dt \qquad (7)$$

Figure 6 compares the experimental and numerical values of Nu_0 of the concave surface under intermittent jet for H/d=2 and 5. The acceptable deviation is observed from the experimental data. The maximum error of the numerical result is acquired at approximately 11% at f=15 Hz and H/d =2. Although the jet is fully turbulent due to the high jet Reynolds number, because of the zero velocity in stagnation, the boundary layer is laminar on the stagnation point. When the distance of the nozzle to the surface increases, the surface is located out of the potential core, and transition doesn't occur on the surface. Therefore, the error for H/d=5 is decreased. According to the figure, all of the numerical results are in the range of uncertainty of experimental data. Consequently, it can be said that the numerical simulation has reasonable accuracy for the whole of the frequency range.

According to the figure, at H/d=2, pulsating the inlet jet with low frequencies of f=1 Hz and 5 Hz decreases the Nu_0 from 78 to 63 and 67, respectively. This reduction happens because the enhanced heat transfer during the half period of jet-on isn't adequate to compensate for the reduced cooling during the jet off [19, 25, and 34]. This behavior continues until f = 50 Hz for H/d = 2 and f =40 Hz for H/d=5.The corresponding threshold Strouhal number of these frequencies are 0.075 and 0.06 for H/d=2 and 5, respectively. It can be concluded that at the low frequency of the pulsation, the Nu number of stagnation point decreases because of the larger period of the pulsation in comparison to the residence time [35-36]. According to Fig.6, pulsating the inlet jet with the frequency of 100 Hz leads to an increase in the Nu_0 by 17% and 12% jet for H/d=2 and H/d=5, respectively. It can be seen from the figure that for f =100 Hz, by increasing the jet to surface distance from H/d=2 to H/d=5, Nu_0 reduces from 91 to 77.

Figure 7 depicts the comparison of the current experimental data with the other research [37]. As observed in the figure, the Nu value for the concave surface is greater than the flat surface for whole jet regions. As seen in the figure, pulsating the inlet jet on concave surfaces is more effective than flat ones in the region of the wall jet. As it was mentioned in other researches [22-24], for flow over the concave surface, the Taylor-Gortler vortices are produced due to the centrifugal force. These vorticities cause the momentum and energy exchange enhancement in the flow, then increase the Nu number. It is observed in Fig.8, pulsating the inlet jet leads to the occurrence of maximum turbulent kinetic energy on the concave surface. The turbulent kinetic energy of the pulsed jet is reached to 12 m^2/s^2 on the concave surface, while this value is 6 m^2/s^2 and 8 m^2/s^2 for the steady jet on the concave surface and pulsed jet on the flat plate, respectively. According to Fig.8, when the frequency of pulsating increases to 100 Hz, the turbulent kinetic energy of the flow increases as compared to the steady jet. Therefore an increase of Nu number is observed with increasing the turbulent kinetic energy.

It can be said that the concave surface and pulsating jet cause heat transfer enhancement by increasing the turbulent intensity of the impinging jet. This observation is consistent with the literature [24-26].
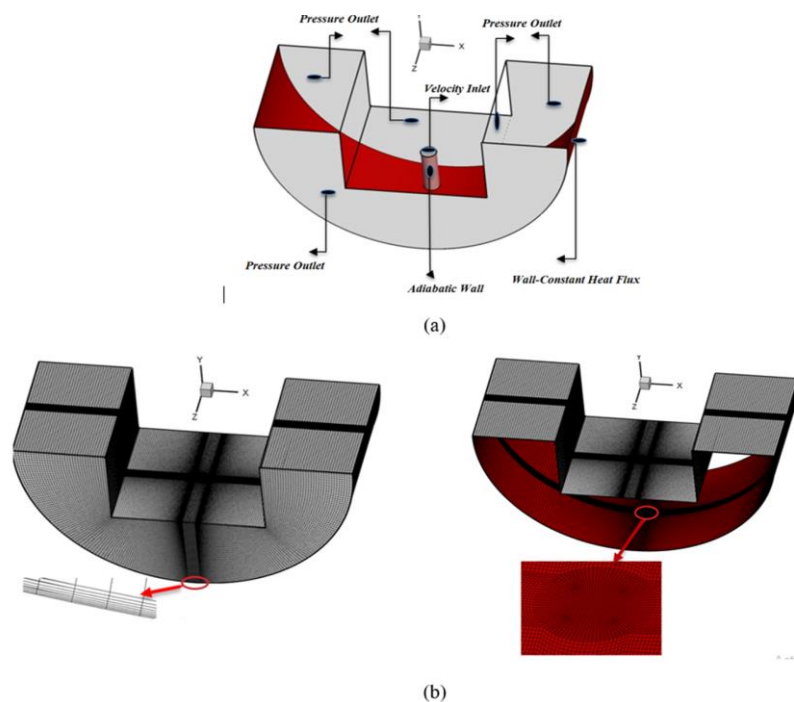
Figure 5. a) Geometry and boundary condition b) Structured and non-uniformed grid
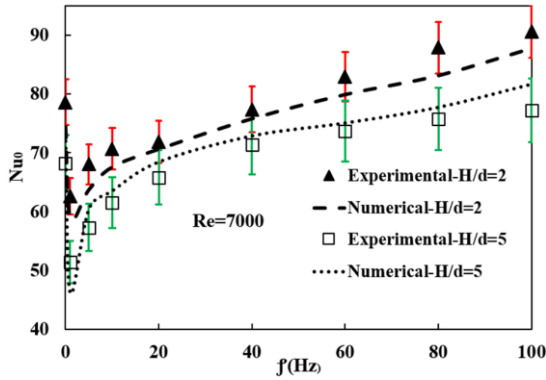
Figure 6. Comparison of experimental and numerical results for the Nusselt number of pulsed jet impinging at the stagnation point
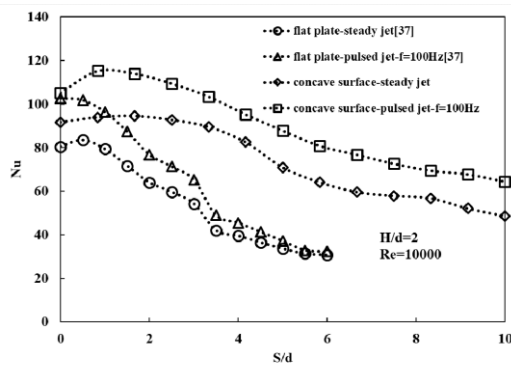
Figure 7. Comparison of Nu distribution on the concave and flat surface for steady and pulsed jet

The effect of low frequencies pulsating on Nusselt distribution is displayed in Fig.9. It is observed that Nusselt distribution for 100 Hz frequency is more than that for two cases of the steady and low-frequency pulsed jet. This is because of the stronger turbulence vorticities of the pulsed jet as compared to the steady jet. As we know, by pulsating the inlet jet, the air entrainment to the jet centerline is increased. It is expected that increasing the air entrainment causes a reduction in Nusselt number. This occurs in low frequency. According to the figure, applying the pulsating by low frequency causes a decrease of the Nu distribution as expected. Raizner et al. [36] found that if the primary vortex frequency of the pulsed jet is higher than a steady jet, pulsating causes the increasing heat transfer rate; otherwise, heat transfer reduction has appeared. Furthermore, the removal of the hydrodynamic boundary layer thickness, conduct to increase of Nu number in the pulsed jet case [12].

According to Fig. 9, the maximum Nu is obtained at S=d and S=2d for the frequency of 100 Hz and low-frequencies (f =1 Hz &5 Hz), respectively. It can be concluded that the width of the stagnation region is s=d for low frequencies while the maximum Nu occurred at the stagnation point for f =100 Hz. The local peaks along with the circumferential and axial directions are strongly determined by the laminar to turbulent transition in

boundary layers. The transition region can be developed along the wall when the concave surface is positioned inside the jet's potential core. The pulsation might cause early transition, which can explain the observed shifts of local heat transfer peaks. This could be due to the deformation of the potential core by pulsating the free jet. Figure 10 demonstrates the velocity distribution of the inlet jet along the jet centerline. The potential core region finishes where the u/U_{jet} =0.97. As seen in the figure, unlike the steady jet, the potential core has been decayed in the pulsed jet. To determine the effects of intermittent pulsation, the characteristic of the pulsed jet should be investigated before impinging to the concave surface. Hence the frequency shedding of the pulsed jet is examined through the contour of Q-criterion [38]. The Q parameter is defined: $\frac{\partial v}{\partial y}\frac{\partial u}{\partial x} - \frac{\partial v}{\partial x}\frac{\partial u}{\partial y}$. According to Fig. 11, the shedding frequency of the pulsed jet is nearly equal to the pulsation frequency as reported in Refs [39-40]. Therefore, increasing in the pulse frequency, leads an increase the shedding frequency.

The time and axial-averaged Nusselt numbers are calculated using experimental data. The impact of pulsating along the axial and circumferential directions can be understood in table.3. According to the table, at H/d=2, pulsating the flow leads to an increase in the averaged Nu by 12% and 4% for f =100 Hz in the axial and circumferential direction, respectively. Therefore, the effect of the pulsed jet along the axial direction is higher than the circumferential. Furthermore, Results show that at H/d=5, pulsating the inlet jet with f =1 Hz, 5 Hz, and 20 Hz decreases the averaged Nu by 18%, 14%, and 4% in the axial direction, respectively. However, these reductions are lower in the curvature direction.

Figure 12 illustrates the effect of Re on the Nu distribution on the concave surface. As it is observed in the figure, the Nu distribution of pulsed impinging jet is compared with a steady jet on the concave surface [41]. It should be noted that experimental data of Ref [41] were performed at Re= 10000 for the steady jet. According to the figure, pulsating the inlet jet leads to an increase in Nu number at stagnation and wall jet region. Furthermore, local Nu increases by an increase in the Re. This behavior is observed in pulsed-jet impinging on flat surfaces [11-13] and steady jets on concave surfaces [22]. This is because the larger Re causes more momentum and turbulence intensity at stagnation also more instability on the wall jet area.

The effect of the distance of the nozzle to the surface on the local Nu distribution is demonstrated in Fig.13. It is seen from the figure that, as the nozzle moves away from the surface (H/d) increases from 2 to 5, the Nu of stagnation point decreases by 12%. It could be mentioned that by increasing the distance of jet to surface, the rate of air entrainment is increased. As the space between the jet and surface increases, the maximum Nu gets closer to the stagnation point. This can be attributed to the rate of entrainment and transition from laminar to turbulent. By

increasing the distance of the jet to the surface, the air entrainment increases [39]. Turbulent intensity is increased when air entrains the jet centerline; therefore, the jet flow reaching the surface is turbulent, and the maximum Nu occurs in stagnation point [43]. It is observed from Fig.13 that the local Nu approaches close values at the end of the surface for the various distances of nozzle to surface. Similar behavior was shown in previous research efforts [25-26]. The temperature distribution has been demonstrated for two nozzle to surface distances in Fig.14. As is observed in the figure, the temperature of the concave surface decreases by applying the pulsation on the steady jet. This observation is also found in Ref [44]. It is seen from the figure that by increasing the distance between the nozzle and the concave surface leads to an increase in the temperature across the concave surface for both jet-on and jet-off states, as observed in previous researches [41. Also, the downstream temperature of the concave surface is high, and the stagnation region width decreases as the jet to surface distance increases.

According to Fig.14, as H/d reduces from 5 to 2, the maximum temperature also drops from 535 K to 472 K. The effect of Reynolds number on Nu of stagnation point is shown in Fig 15. There is a direct relation between the Reynolds number and Nusselt number, as expected. Increasing the Reynolds number, leads to an increase in the impinging velocity of the half of the cycle. This leads

to creating the recirculation zone (see Fig.8) in the second part of the cycle, and consequently, the Nusselt number of stagnation increases [22, 40]. For H/d=2, Nu increases by 30% when the Re number rises from 7000 to 14000. For the same increase in the Re, the enhancement percentages are 18% and 12% for H/d=4 and 5, respectively.

Fig.16 depicts the impact of the nozzle to concave surface distance on the Nu number of stagnation point. It is seen from the figure that the Nusselt of stagnation point decreases as the nozzle to surface spacing increases. This may be because ambient air reaches the centerline of the jet before impinging on the surface (see Fig. 10). According to the figure, the slope of the Nusselt number curve is reduced as we move from the lower nozzle to surface distances to higher ones [22]. The Nu_0 is independent of the distance of the jet to surface for H/d>4 because the concave surface is out of the potential core of the impingement jet [41, 44]. The Nu variation of stagnation point with low and high Strouhal numbers is demonstrated in Fig.17. It is observed that by increasing the Sr, the Nu_0 increases for both ranges of Sr. Also, Nu variation is sharper for larger values of Sr. According to the figure for H/d=2, Nu_0 varies with $Sr^{0.05}$ and $Sr^{0.15}$ for the low and high frequencies, respectively. From the literature, Hsu [45] found that Nu varies with $Sr^{0.019}$ for the pulsed impinging jet on the flat surface.
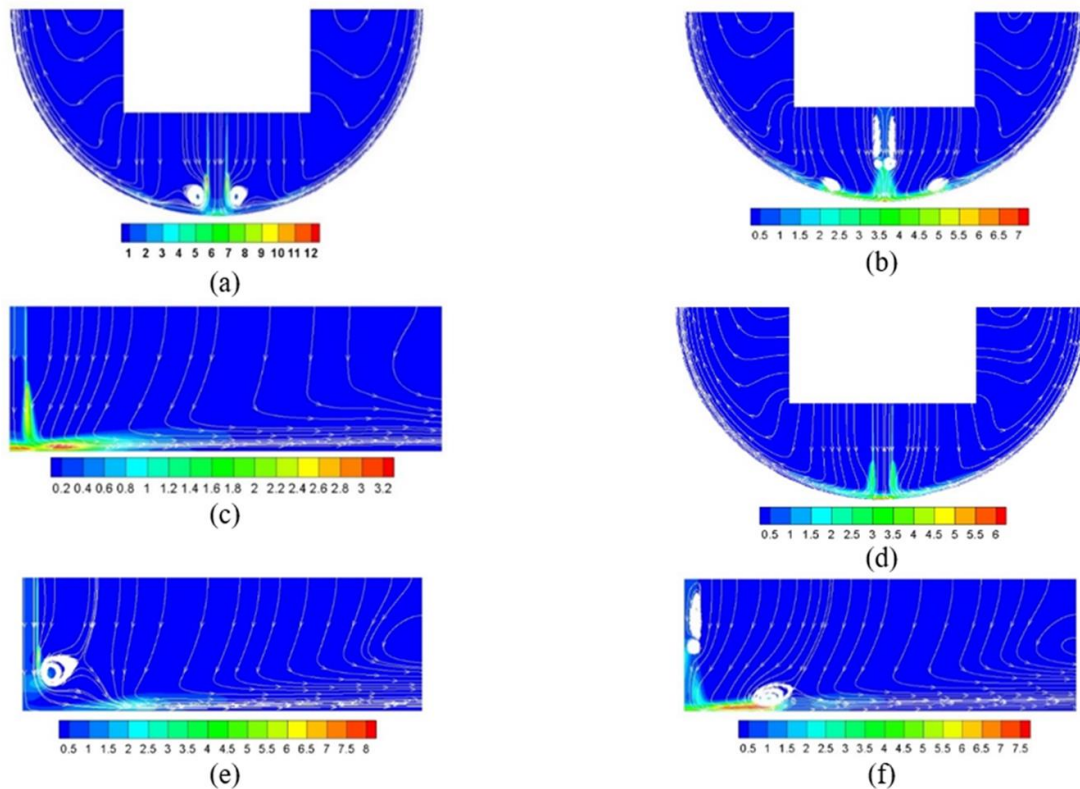
Figure 8. The contour of turbulent kinetic energy, Re=7000, *f*=100 Hz (for the pulsed jet), a) concave surface-jet on, b) concave surface-jet off c) flat plate-steady jet, d) concave surface-steady jet, e)flat plate-Jet on, f)flat plate Jet off
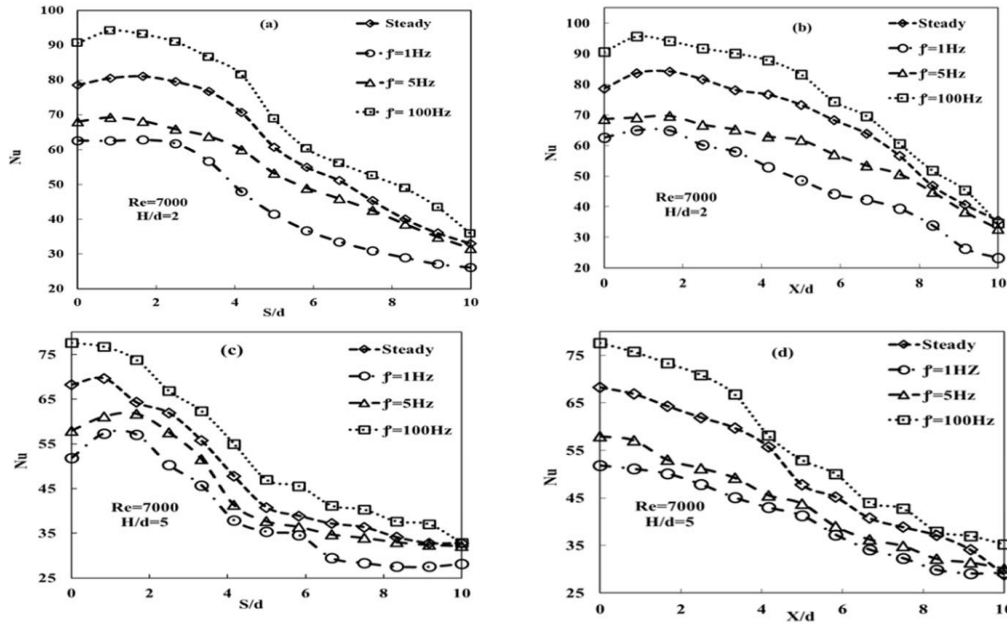
Figure 9. Nu Profile on the concave surface under Pulsed Impinging jet along (a, c) circumferential and (b, d) axial Directions
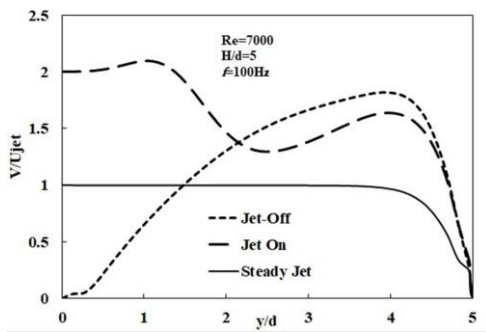
Figure 10. Vertical velocity distribution over the jet centerline for pulsed and steady jet

The impact of frequency of pulsed jet on time and area-averaged Nu number is investigated, and the results are presented in Table 4. The time and area-averaged Nusselt number is obtained as follows:

$$\overline{Nu}_{ave} = \frac{1}{100\pi d^2} \frac{1}{T} \int_{-5d}^{5d} \int_{0}^{T} Nu(x.\theta.t)dx.d\theta.dt \tag{8}$$

Accordingly, an enhancement in the total-averaged Nusselt number is found with increasing frequency. The intermittent jet with a pulse frequency of 100 Hz improve the time and area-averaged Nusselt numbers by 22% and 20% related to the steady jet at the nozzle to surface distance of 2 and 5, respectively. The corresponding values for Re=7000 are 15% and 13%, respectively. Furthermore, pulsating the inlet jet with low frequencies (i.e. f =1 Hz and 5 Hz) leads to a decrease in the Nu$_{ave.}$
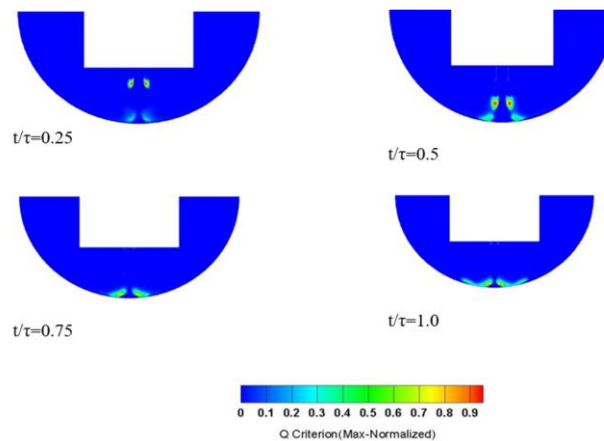
Figure 11. The contour of Q-criterion
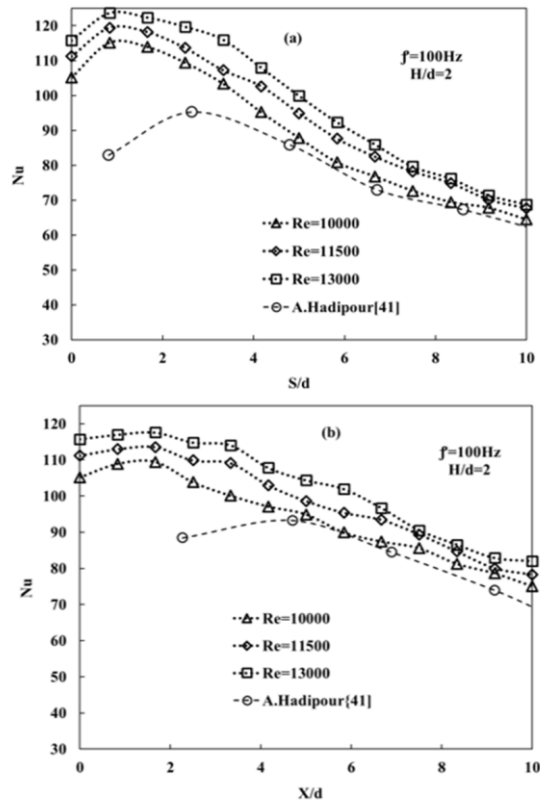
Fig. 12 Effect of Reynolds number on the Nu distribution across the concave surface under the intermittent jet along (a) circumferential and (b) axial Directions
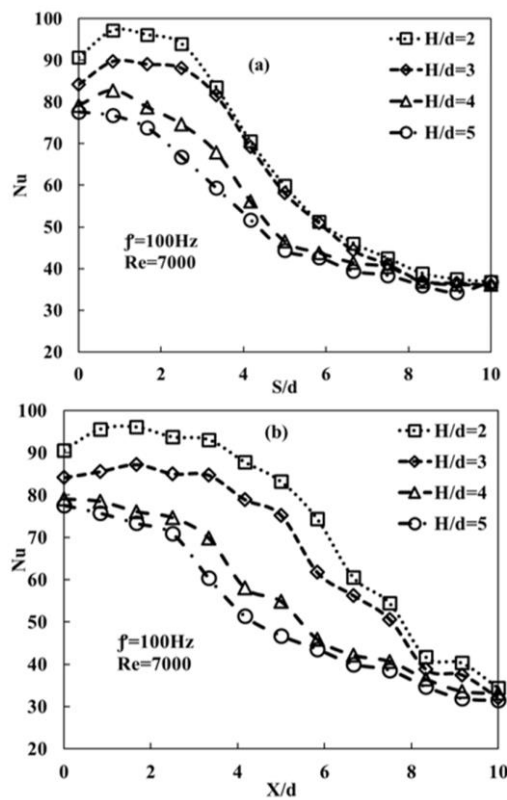
Figure 13. Effect of the nozzle to the surface distance on the Nu distribution across the concave surface under the intermittent jet along (a) circumferential and (b) axial Directions.

Table 3. Time and axial averaged Nusselt number for pulsed and steady jet impinging on the concave surface (Re=7000)

H/d	Direction	Steady	$f=1$ Hz	$f=5$ Hz	$f=20$ Hz	$f=60$ Hz	$f=100$ Hz
5	X	49.82	40.19	42.30	47.70	53.40	54.03
	S	46.44	41.80	44.60	45.70	50.64	52.15
2	X	64.64	46.16	57.09	66.70	68.60	72.79
	S	61.26	44.41	54.05	63.70	63.83	64.69
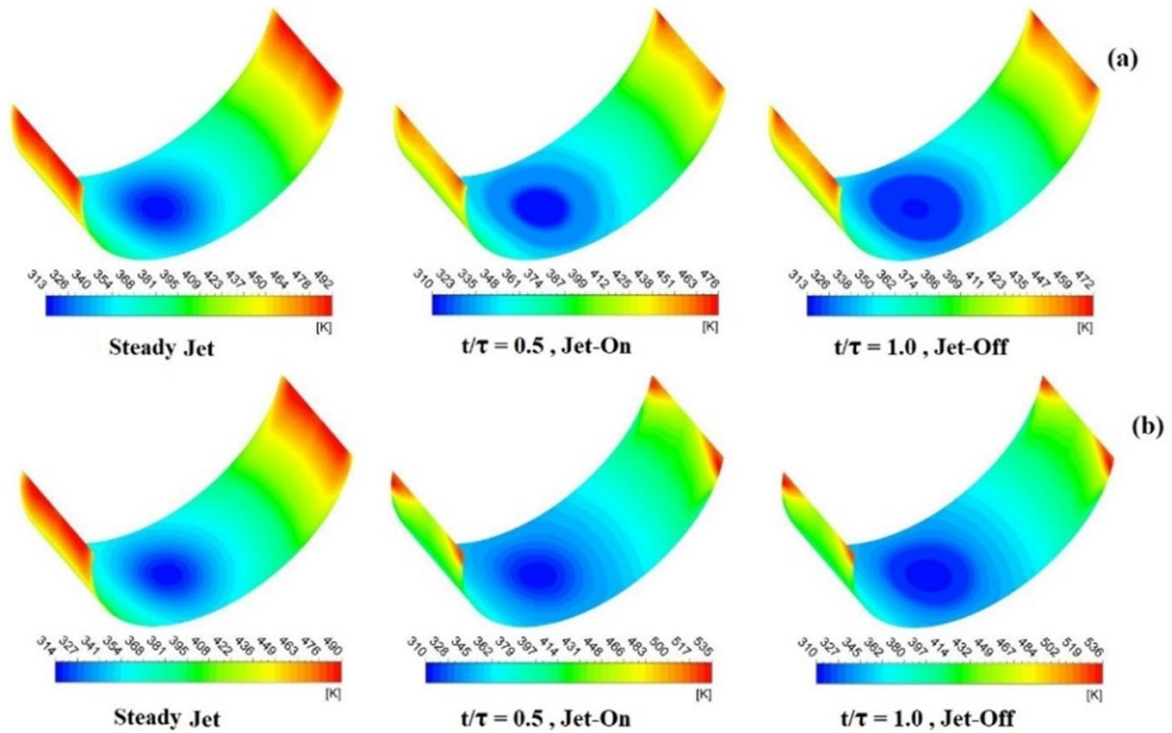
Figure 14. Effect of the nozzle to the surface distance on temperature distribution across the concave surface (Re=7000, f=100 Hz) (a) H/d=2, (b) H/d=5
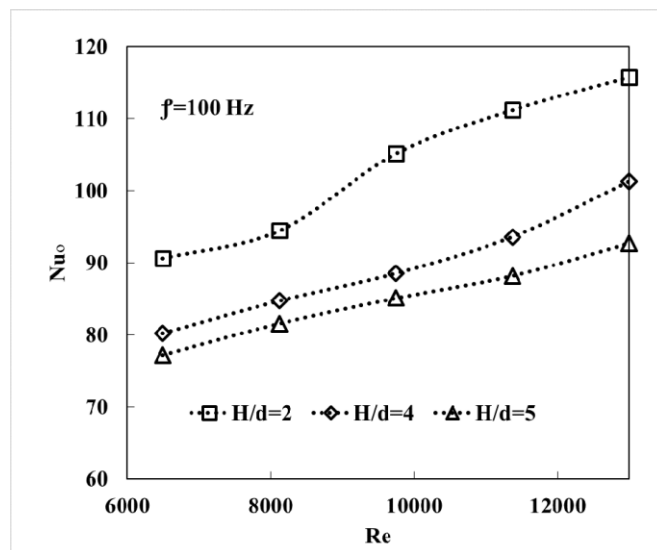
Fig 15. Effect of Reynolds Number on the Nu_0
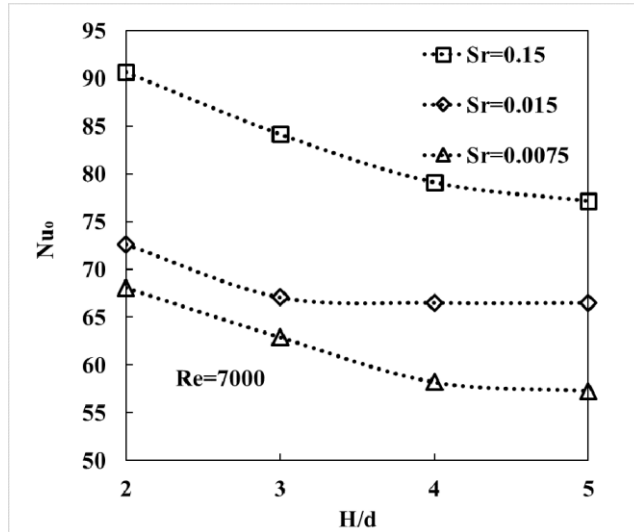
Figure 16. the nozzle to surface distance effect of on the Nu_0
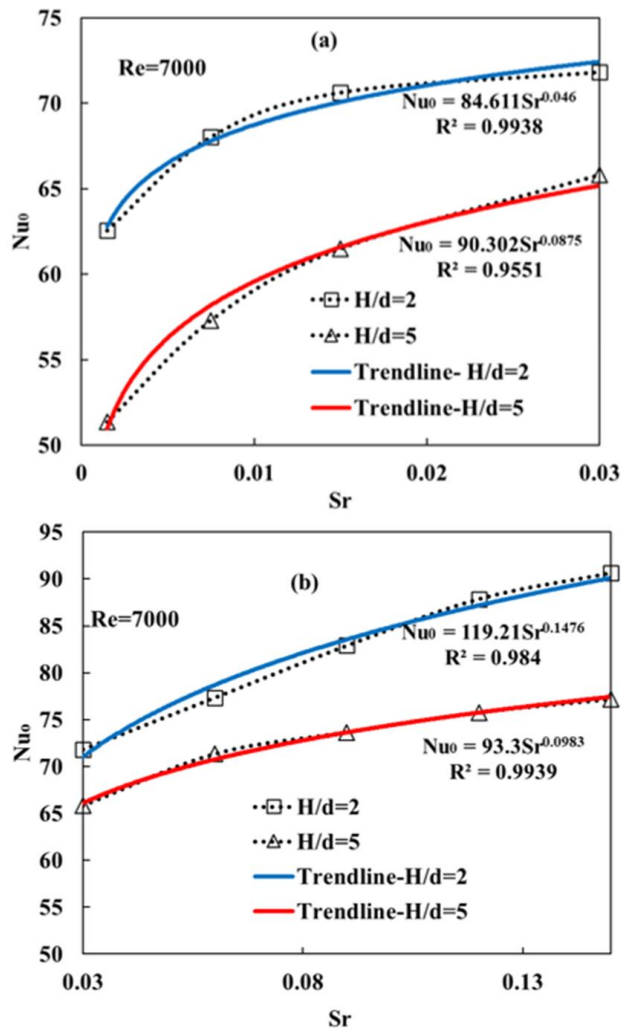
Figure 17. Variation of Nu of stagnation point with Strouhal Number a) Low Strouhal number b) High Strouhal Number

Table 4. Effect of frequency of pulsed jet on the Nu_{ave}

Re	H/d	Steady	f =1 Hz	f =5 Hz	f =50 Hz	f =60 Hz	f =80 Hz	f =100 Hz
7000	5	62.84	58.28	58.66	65.51	67.73	68.33	70.25
	2	64.21	60.82	62.15	68.20	68.30	69.08	74.03
10000	5	65.74	63.64	64.06	73.38	75.86	76.53	78.68
	2	68.97	67.03	67.58	79.11	79.23	80.13	83.55

Conclusion

Numerical and Experimental investigations have been performed to study the flow field and heat transfer from a pulsed jet impinging on a concave surface. Hence the pulsed jet generator has been manufactured using a disc that has been perforated as two arcs 90 degrees symmetrically. The pulsed velocity of the jet was measured using a pitote tube equipped with an A/D card. The temperature of the black concave surface has been measured by an IR camera. The effect of the pulse frequency, Reynolds number, and nozzle to surface distance on the distributions of Nusselt number are accordingly studied. The effect of the pulsating jet and concave surface on the flow structure of the impinging jet has been studied through numerical simulation. The major acquired findings can be listed as below:

- The Numerical results and experimental data show that pulsating the impinging jet significantly affects the Nu distribution along with both S and X directions.
- At frequencies larger than the threshold frequency, pulsating the impinging jet leads to an increase in the Nu distribution.
- Numerical simulation showed that the turbulent kinetic energy of pulsating the inlet jet on the concave surface produces more turbulent kinetic energy than steady impinging jet on the flat and concave surface.
- The excited frequency of the inlet jet determines the shedding frequency of flow of the pulsed impinging jet.
- The potential core of impinging jet is decayed by applying the pulsating on the jet.
- For the pulsed jet impinging to the concave surface, threshold Strouhal numbers are Sr=0.075 and 0.03 for H/d=2 and 5, respectively.
- At low frequencies (f =1 Hz and 5 Hz), Nu_{ave} of the pulsed jet is reduced related to the steady jet by 8% and 5%, respectively.
- Pulsating the inlet jet with f =100Hz leads to an increase in the Nu_{ave} by 15% and 13% at H/d=2 and 5, respectively.
- According to the results, Nu_0 respectively varies with $Sr^{0.05}$ and $Sr^{0.15}$ for low and high frequencies.

Nomenclature

H	Specific enthalpy [KJ/Kg]
I	Exergy destruction rate [KJ/Kg]
M	Mass flow rate [Kg/s]
P	Pressure [bar]
c_p	specific heat
d	diameter of the nozzle
H	nozzle-to-surface distance
h	convection heat transfer factor
K	Thermal conductivity
k	turbulence kinetic energy
$\bar{U}_{jet}$	Averaged Jet velocity
Nu=hd/λ	time-averaged of local Nusselt number
Nu_{ave}	time and area-averaged of Nusselt number
Sr= fd/ $\bar{U}_j$	Strouhal Number
P	static pressure
q''	heat flux
T	temperature
T_s	Surface temperature
T_{jet}	jet air temperature
t	time
u	velocity in x- direction
v	velocity in x- direction
w	velocity in x- direction
x_i	coordinates (x, y, z)
Y+	dimensionless distance
ε	turbulent dissipation rate
μ	dynamic viscosity
λ	Thermal conductivity
ρ	density
τ	period of pulsed jet
$\square$	frequency of pulsed jet

References

[1] A. Hadipour, M. Rajabi Zargarabadi, M. Dehghan, Effect of micro-pin characteristics on flow and heat transfer by a circular jet impinging to the flat surface, Journal of Thermal Analysis and Calorimetry, 140, 943–951, (2020).

[2] H. Ramezanzadeh, A. Ramiar, M.Yousefifard, M. Ghasemian, Numerical analysis of sinusoidal and step pulse velocity effects on an impinging jet quenching Process, Journal of Thermal Analysis and Calorimetry, 140,331–349, (2020).

[3] M. Ataei, R. Tarighi, A. Hajimohammadi, M. Rajabi zargarabadi, Heat Transfer under Double Turbulent Pulsating Jets Impinging on a Flat Surface, Journal of Heat and Mass Transfer Research, 4, 45-52,(2017).

[4] R. V. Hout, V. Rinsky, Y. G. Grobman, Experimental study of a round jet impinging on a flat surface: Flow field and vortex characteristics in the wall jet, Int. J. Heat and Fluid Flow, 70, 41-58,(2018).

[5] P. Xu, A. P. Sasmito, S. Qiu , A. S. Mujumdar , L. Xu, L. Geng, Heat transfer and entropy generation in air jet impingement on a model rough surface, International Communications in Heat and Mass Transfer, 72, 48–56, (2016).

[6] H. Ramezanzadeh, A. Ramiar, M. Yousefifard, Numerical analysis of sinusoidal and step pulse velocity effects on an impinging jet quenching process, J Therm Anal Calorim, 140, 331–349 (2020).

[7] M. Haines, I. Taylor, The turbulence modelling of a pulsed impinging jet using LES and a divergence free mass flux corrected turbulent inlet, Journal of Wind Engineering and Industrial Aerodynamics, 188, 338-364, (2019).

[8] P. Xu, S. Qiu, M. Zhou Yu, X. Qiao, A. S. Mujumdar, A study on the heat and mass transfer properties of multiple pulsating impinging jets, International Communications in Heat and Mass Transfer, 39, 378–382, (2012).

[9] T. Ikeda, Y. Mori, Y. Tsuchiya, T. Nagasawa, T. Horikosi, A Study on Pulsating Jet (Observation on the Behavior of the Vortices by Means of Flow Visualization), Journal of the Visualization Society of Japan, 17(67), 292-297, (1997).

[10] D. J. Sailor, , J.R. Daniel, F. Qianli, Effect of Variable Duty Cycle Flow Pulsations on Heat Transfer Enhancement for an Impinging Air Jet, Int. Journal of Heat and Fluid Flow,20, 574-580, (1999).

[11] H. J. Poh, K. Kumar, A.S. Mujumdar, Heat transfer from a pulsed laminar impinging jet, Int. Communications in Heat and Mass Transfer, 32, 1317-1324, (2005).

[12] X. Peng, A. S. Mujumdar, P. H. Joo and Y. Boming, Heat transfer under a pulsed slot turbulent impinging jet at large temperature differences, Thermal science, 14(1), 271-281, (2010).

[13] R.C Bejera, P. Dutta, K.Srinivasan, Numerical Study of Interrupted Impinging Jets for Cooling of Electronics, IEEE Transactions on Components and Packaging Technologies, 30(2), 275-284, (2007).

[14] J.W. Zhou, G. Wang, G. Middelberg, H. Herwig, Unsteady jet impingement: heat transfer on smooth and non-smooth surfaces, Commun Heat Mass Transf, 36,103–110. (2008).

[15] J. C. Kurnia, A. P. Sasmito P. Xu, A. S. Mujumdar, Performance and potential energy saving of thermal dryer with intermittent impinging jet, Applied Thermal Engineering,113, 246-258, (2017).

[16] H.J. Poh, and A.S. Mujumdar, Heat Transfer from a Pulsed Turbulent Impinging Jet at Large Temperature Differences, Proceedings, 5 th Asia-Pacific Drying Conference, Hong Kong, 1171-1177, (2007).

[17] G. Middelberg, and H. Herwig. Convective heat transfer under unsteady impinging jets: the effect of the shape of the unsteadiness, Heat Mass Transfer, 45, 1519–1532, (2009).

[18] R. Zulkifli, K. Sopian, S. Abdullah, and M.S. Takriff, Comparison of local Nusselt number for steady and pulsating circular jet at Reynolds number of 16000, European Journal of Scientific Research, 29, 369-378, (2009).

[19] J. Mohammadpour, M. Zolfagharian, A. S. Mujumdarb, M. Rajabi Zargarabadi, M. Abdula Hzadeh, Heat transfer under composite arrangement of pulsed and steady turbulent submerged multiple jets impinging on a flat surface, International Journal of Thermal Sciences, 86, 139-147, (2014).

[20] S. M. Hosseinalipour, S. Rashidzadeh, M. Moghimi, K. Esmailpour, Numerical study of laminar pulsed impinging jet on the metallic foam blocks using the local thermal non-equilibrium model, Journal of Thermal Analysis and Calorimetry, (2019).

[21] H. Eren, N. Celik, B. Yesilata, Nonlinear flow and heat transfer dynamics of a slot jet impinging on a slightly curved concave surface, International Communications in Heat and Mass Transfer, 33, 364–371, (2006).

[22] Z. Ying, L.Guiping, B. Xueqin, B. Lizhana, W.D. Shenga, Experimental study of curvature effects on jet impingement heat transfer on concave surfaces, Chinese Journal of Aeronautics, 30, 586-594, (2017).

[23] J. Taghinia, M. Rahman, T. Siikonen, Heat transfer and flow analysis of jet impingement on concave surfaces, Applied Thermal Engineering, 84, 448-459, (2015).

[24] A. Hashiehbaf, A. Baramade, A. Agrawal, G.P. Romano, Experimental investigation on an axisymmetric turbulent jet impinging on a concave surface, International Journal of Heat and Fluid Flow, 53, 167–182, (2015).

[25] J. Mohammadpour, M. Rajabi-Zargarabadi, A. S.Mujumdar, H. Ahmadia, Effect of intermittent and sinusoidal pulsed flows on impingement heat transfer from a concave surface, International Journal of Thermal Sciences, 76, 118-127, (2014).

[26] M. Rajabi, E. Rezaei, B.Yousefi, Numerical analysis of turbulent flow and heat transfer of sinusoidal pulsed jet impinging on an asymmetrical concave surface, Applied Thermal Engineering, 128, 578-585, (2018).

[27] D. Qiu, C. Wang, L. Luo, S. Wang, Z. Zhao, Z. Wang, On heat transfer and flow characteristics of jets impinging onto a concave surface with varying jet arrangements, Journal of Thermal Analysis and Calorimetry, (2019).

[28] S.J. Kline, F.A. McClintock, Describing uncertainties in single sample experiments, Mech. Eng. 75, 3–8, (1953).

[29] N. Kharoua, L. Khezzar, Z. Nemouchi, M. Alshehhi, LES study of the combined effects of groups of vortices generated by a pulsating turbulent plane jet impinging on a semi-cylinder, Applied Thermal Engineering, 114, 948-960, (2017).

[30] C.G. Speziale, S. Thangam, Analysis of an RNG based turbulence model for separated flows, International Journal of Engineering Science, 30, 1379-1388, (1992).

[31] H Ahmadi, M Rajabi-Zargarabadi, A.S. Mujumdar, J Mohammadpour, Numerical modeling of turbulent semi-confined slot jet impinging on a concave surface, Thermal Science, 19(1), 129-140, (2015).

[32] E. Öztekin , O. Aydin , M. Avci, Heat transfer in a turbulent slot jet flow impinging on concave surfaces, International Communications in Heat and Mass Transfer, 44, 77–82, (2013).

[33] S.V. Patankar, Numerical Heat Transfer and Fluid Flow, Hemisphere Publishing, Company. (1980).

[34] M. A. Pakhomov, V. J. Terekhov, Numerical study of fluid flow and heat transfer characteristics in an intermittent turbulent impinging round jet, International Journal of Thermal Sciences, 87, 85-93, (2015).

[35] H.M. Hofmann , D. L. Movileanu , M. Kind, H. Martin Influence of a pulsation on heat transfer and flow structure in submerged impinging jets, International Journal of Heat and Mass Transfer, 50, 3638–3648, (2007).

[36] M. Raizner, V. Rinsky, G. Grossman, R. van Hout, Heat transfer and flow field measurements of a pulsating round jet impinging on a flat heated surface, International Journal of Heat and Fluid Flow, 77, 278–287, (2019).

[37] S. Rakhsha, M. Rajabi Zargarabadi, and S. Saedodin, Experimental and numerical study of flow and heat transfer from a pulsed jet impinging on a pinned surface, EXPERIMENTAL HEAT TRANSFER, (2020).

[38] C. Braud, A. Liberzon, Real-time processing methods to characterize streamwise vortices, Journal of Wind Engineering & Industrial Aerodynamics, 179, 14–25, (2018).

[39] H. Yadav, A. Agrawal, A. Srivastava, Mixing and entrainment characteristics of a pulse jet, International Journal of Heat and Fluid Flow, 61, 1–13, (2016).

[40] S. Ghadi, K. Esmailpour, S.M. Hosseinalipour, A. S. Mujumdar, Experimental study of formation and development of coherent vortical structures in pulsed turbulent impinging jet, Experimental Thermal and Fluid Science,74, 382-389, (2016).

[41] A. Hadipour, M. Rajabi Zargarabadi, Heat transfer and flow characteristics of impinging jet on a concave surface at small nozzle to surface distances, Applied Thermal Engineering, 138, 534-541, (2018).

[42] R.B. Kalifa, S. Habli , N. Mahjoub Saïd ,H. Bournot ,G. L. Pale, Parametric analysis of a round jet impingement on a heated plate, International Journal of Heat and Fluid Flow, 57, 11-23, (2016).

[43] L. A. Brignoni, S. V. Garimella, Effects of nozzle-inlet chamfering on pressure drop and heat transfer in confined air jet impingement, International Journal of Heat and Mass Transfer,43,1133-1139, (2000).

[44] M.A.R. Sharif, K.K. Mothe, Parametric study of turbulent slot-jet impingement heat transfer from concave cylindrical surfaces, International Journal of Thermal Sciences, 49, 428–442, (2010).

[45] C. M. Hsu, W. C. Jhan, Y. Y. Chang, Flow and heat transfer characteristics of a pulsed jet impinging on a flat plate, Heat and Mass Transfer, (2019).